1   Competition-driven growth of Atka mackerel in the Aleutian Islands ecosystem revealed by

2   an otolith biochronology

3

4

5   Mary Elizabeth Matta[1]*, Kimberly M. Rand[2], Morgan B. Arrington[3], Bryan A. Black[4]

6

7   [1]Resource Ecology and Fisheries Management Division, Alaska Fisheries Science Center,

8   National Marine Fisheries Service, National Oceanic and Atmospheric Administration, 7600

9   Sand Point Way NE, Seattle, WA 98115, USA

10   [2]Lynker Technologies, LLC, 202 Church Street SE #536, Leesburg, VA 20175, USA

11   [3]School of Aquatic and Fishery Sciences, University of Washington, 1122 Boat Street, Seattle,

12   WA 98195, USA

13   [4]Laboratory of Tree-Ring Research, University of Arizona, 1215 E. Lowell Street, Tucson, AZ

14   85721, USA

15

16   *corresponding author

17

18   **Abstract**

19

20   Fish otolith increment biochronologies can reveal factors contributing to growth. These annually

21   resolved, multi-decadal biochronologies have been used to identify temporal and spatial patterns

22   in growth variability. Here, we used a linear mixed modeling approach to determine the relative

23   importance of intrinsic factors (e.g., sex, age) and extrinsic factors (e.g., temperature, abundance

24   of con-specifics and competitors) to growth of Atka mackerel (*Pleurogrammus monopterygius*),

25   a commercially important groundfish dominant in the Aleutian Islands ecosystem. A yearly

26   alternating pattern of wide and narrow increments was observed, and was negatively correlated

27   with abundance of pink salmon (*Oncorhynchus gorbuscha*), suggesting possible competition

28   over shared food resources such as large copepods (which were positively correlated with the

29   otolith biochronology). There was no detectable effect of temperature on otolith growth, which

30   could be a result of relative stability in water temperatures at the study site. We also contrast the

31   otolith biochronology with a body condition index to examine the relationship between otolith

32   and somatic growth. This represents the first otolith biochronology developed in the Aleutian

33   Islands and provides insight into potential species interactions and their impacts on growth

34   within this highly dynamic and productive ecosystem.

35

36

37

38   **Keywords:** Sclerochronology, Growth, Aleutian Islands, Body condition, Competition, Otolith

1. Introduction

Describing growth of individuals is essential for understanding fish population dynamics, particularly as a rising number of studies have recognized the potential for growth to vary over time (Stawitz et al., 2015; Lorenzen, 2016). Variability in growth is driven by a suite of inherent factors such as ontogenetic development and extrinsic factors, including environmental conditions, food availability, and competition for shared resources, all of which can vary across space and time (Walters and Wilderbuer, 2000; Sibley et al., 2015; Morais and Bellwood, 2018). Understanding past relationships between these factors and growth may aid with predicting future effects on growth resulting from changes in the external physical and biological environments to which a group of individuals is exposed. Given the level of climate change projected to occur in many marine environments and subsequent cascading impacts on ecological communities (Wang et al., 2010; Oliver et al., 2019), such information is highly relevant to fisheries managers.

An increasing number of studies have used increment widths formed in the hard structures of marine organisms, such as fish otoliths, to develop biochronologies as proxies for somatic growth over time (Black et al., 2008; Morrongiello et al., 2012). Otoliths grow continuously over the life of a fish, and the relative widths of their annual increments are often related to variability in oceanographic and biotic factors (Black et al., 2011; Doubleday et al., 2015; Ong et al., 2018). The dendrochronology (tree-ring science) technique of crossdating ensures that increments have been assigned the correct year of formation and thereby eliminates even modest dating errors that can severely mute environmental signals, especially in long-lived species (Black et al., 2016). Crossdating becomes more challenging in shorter-lived species (< 15

62 yr) due to the lack of overlap among samples, but can still be highly effective when interannual

63 variability in growth is high (Matta et al., 2010). Once increments are dated and measured,

64 mixed effects modeling offers a flexible approach for directly evaluating the magnitude of

65 intrinsic effects, such as sex or fish age, and extrinsic effects, such as temperature or prey

66 abundance, on otolith growth (Helser et al., 2012; Morrongiello and Thresher, 2015). Moreover,

67 otolith biochronologies often predate instrumental records, allowing an extended window into

68 past environmental conditions (van der Sleen et al., 2016). As biochronology techniques are

69 more widely implemented, a global library of datasets is emerging that can inform us of

70 covariability across instrumental records, diverse taxa, and trophic levels that may inform

71 species' responses to projected climate change (Barrow et al., 2018; Black et al., 2019).

72   Particularly well-suited to biochronology studies are species that utilize localized habitats

73 and that possess clear growth increments. Atka mackerel (*Pleurogrammus monopterygius*) is a

74 commercially and ecologically important species endemic to the North Pacific Ocean for which

75 archived otoliths from survey and fishery collections exist (Anderl, 2012). Long-term tagging

76 studies indicate that Atka mackerel have relatively small home ranges, rarely migrating more

77 than 50 km outside their local aggregations (McDermott et al., 2005, 2016). Although Atka

78 mackerel are found in small aggregations elsewhere, the population epicenter remains focused

79 within the U.S. Aleutian Islands (Lauth et al., 2007b), likely due to the region's unusual

80 oceanographic dynamics. The Aleutian Islands, an active volcanic chain, act as a natural barrier

81 that separates the Bering Sea to the north and the Pacific Ocean to the south (Fig. 1). The

82 dominant climatic feature of the Aleutian Islands is the Aleutian Low, a low-pressure system that

83 is the primary driver of temperature variation in the region, varies on interannual to interdecadal

84 timescales, and is teleconnected to the El Niño Southern Oscillation (Rodionov et al., 2005;

85   O'Reilly, 2018). In the central U.S. Aleutian Islands lies Seguam Pass (Fig. 1), the site of one of

86   the most consistently dense aggregations of Atka mackerel, likely due to its strong vertical

87   mixing and swift bottom currents (Rand et al., 2019). Compared to other large marine

88   ecosystems in Alaska such as the Bering Sea and Gulf of Alaska, the Aleutian Islands are not as

89   well-studied, and constructing an otolith biochronology from a key species in this region may

90   allow insight into underlying environmental and biological dynamics.

91   The objective of our study was to identify key drivers of growth of Atka mackerel that

92   involve not only physical variables, but also biological indicators of ecosystem functioning. To

93   accomplish this, we developed an otolith growth time series based on Atka mackerel caught in

94   Seguam Pass, the portion of the Aleutian Islands where this species is most locally abundant. We

95   used a mixed modeling approach to explicitly determine the relative impacts on growth of

96   intrinsic factors such as sex or age, as well as extrinsic factors such as environmental variability,

97   competition, and food resources. We had the unique opportunity to include not only indices of

98   climate but also abundance time series of zooplankton, a major prey group, and pink salmon

99   (*Oncorhynchus gorbuscha*), a potential competitor, to provide an ecosystem-level perspective.

100   Finally, we compared anomalies in otolith growth to independent estimates of body condition to

101   test the otolith biochronology's viability as a proxy for somatic growth, an aspect that has rarely

102   been examined in previous biochronology studies. This Atka mackerel otolith biochronology

103   represents the first such index developed from the Aleutian Islands region, with the overarching

104   goal of providing information regarding relationships among oceanographic and biological

105   variables within this highly dynamic and productive large marine ecosystem.

106

107

108   **2. Materials and methods**

109

110   *2.1 Study species, collection area, and sample selection*

111   Atka mackerel is a member of the greenling family (Hexagrammidae) and is one of the

112   most abundant groundfish species in the U.S. Aleutian Islands. Atka mackerel form large, dense

113   aggregations often in areas of high current velocity (McDermott et al., 2005; Lauth et al., 2007b)

114   and undergo diel vertical migrations, rising in the water column during daytime hours,

115   presumably to feed on pelagic zooplankton (Nichol and Somerton, 2002). Atka mackerel are

116   considered primarily zooplanktivores (Yang, 1999; Rand et al., 2010); however, fish

117   consumption (mostly smelts) has been shown to increase during the summertime months,

118   especially in the central portion of the Aleutian Islands (Rand et al., 2010). Although Atka

119   mackerel diets can be quite diverse, in general, euphausiids and pelagic calanoid copepods are

120   the dominant components (Yang, 1999; Rand et al., 2010). Atka mackerel are considered

121   important prey to several fish species in the Aleutian Islands, including Pacific cod (*Gadus*

122   *macrocephalus*), Pacific halibut (*Hippoglossus stenolepis*), and arrowtooth flounder (*Atheresthes*

123   *stomias*) (Yang, 1999), as well as a large marine mammal, the Steller sea lion (*Eumetopias*

124   *jubatus*) (Sinclair et al., 2005). Similar to other hexagrammids, their reproductive strategy is

125   somewhat unique in that males guard nests of eggs on the ocean floor for extended periods of

126   time (up to three months) (Lauth et al., 2007b). The spawning season lasts from late June to mid-

127   October, peaking in September (McDermott and Lowe, 1997; Lauth et al., 2007a). Atka

128   mackerel populations reach 50% sexual maturity at 3.6 years (McDermott and Lowe, 1997;

129   Cooper et al., 2010) and have a maximum observed age of 15 years (Anderl, 2012).

130   Seguam Pass, located in the central Aleutian Islands, is relatively shallow, dominated by

131   waters from the Alaskan Stream current and is ecologically important (Ladd et al., 2005; Mordy

132   et al., 2005; Zador and Ortiz, 2018). Within the vicinity of Seguam Pass, one of the largest and

133   most persistent aggregations of Atka mackerel supports a large commercial fishery (Lowe et al.,

134   2017) and is the primary prey for Steller sea lion (Sinclair et al., 2005, 2013). Some unique

135   features of Seguam Pass are a north-south temperature dipole, strong flow dominated by tidal

136   currents, and strong vertical mixing that transports nutrients to the upper water column (Stabeno

137   et al., 2005). The northern portion of Seguam Pass is characterized by deepwater upwelling and

138   is often the site of anomalously high chlorophyll-a measurements (Mordy et al., 2005), which in

139   turn correlate with abundance of oceanic zooplankton such as *Neocalanus* and *Eucalanus*

140   copepods and the euphausiid *Euphausia pacifica* (Coyle, 2005), species common in the Atka

141   mackerel diet (Yang, 1999, 2003).

142   Otoliths were collected by fishery observers on commercial vessels actively targeting

143   Atka mackerel in the vicinity of Seguam Pass (within NMFS Statistical Area 541) in the years

144   1996, 1998, 2000, 2002, 2005, 2008, 2010, and 2015 (Fig. 1). Otoliths were randomly selected

145   for growth-increment analysis from fish aged 5 years or older (von Biela et al., 2015). Only

146   otoliths with sufficiently clear growth patterns were retained to ensure precision of growth-

147   increment measurements. A minimum of 30 otoliths per collection year were included in the

148   growth-increment analysis, with collection years spaced no longer than 5 years apart, to ensure

149   adequate replication and overlap of otolith growth-increment time series.

150

151 *2.2 Otolith analysis*

152   Otoliths were snapped in half along the transverse plane and gently burned over an

153 alcohol flame to enhance the contrast between opaque and translucent growth zones (Anderl,

154 2012). Otolith annuli were enumerated during routine production age determination according to

155 protocols established by the Alaska Fisheries Science Center (Anderl, 2012). Atka mackerel do

156 not form a visible annulus during the first year of life (Anderl et al., 1996), so one year was

157 added to all age estimates. Otoliths were illuminated with reflected light from a dual gooseneck

158 LED light source and photographed with a digital camera attached to a Leica MZ9.5

159 stereomicroscope. Starting from the otolith edge and working towards the core, each increment

160 was dated with its year of formation based on capture date and age. Using Image-Pro Premier

161 image analysis software (Media Cybernetics), a measurement axis was drawn perpendicular to

162 each growth zone through the ventral side of the sectioned otolith and increments were

163 delineated distal to each translucent growth zone (Fig. 1). The location of the measurement axis

164 was consistent among specimens. The final increment at the otolith edge was not measured if it

165 was still in the process of forming. Because the first visible increment forms during the second

166 year of life, the portion of the otolith prior to the first increment was not measured. Otolith

167 growth increment measurements from individual fish were then plotted separately relative to fish

168 age at the time of increment formation and to calendar year of formation to evaluate patterns in

169 growth with respect to ontogenetic development and to produce raw growth-increment time

170 series (Fig. 2).

171   Individual growth-increment time series were too short to perform true crossdating.

172 Crossdating is a common practice in biochronology studies whereby synchronous patterns of

173 anomalously wide or narrow increments are matched among individuals (Douglass, 1920). This

174 procedure ensures the annual resolution of each measurement time series and that the final

175 growth-increment dataset is annually resolved and preserves environmental signals. High-

176 frequency variability is especially vulnerable to loss in the absence of crossdating. While an

177 alternating pattern of wide and narrow increments was noted in many individuals (Fig. 1), Atka

178 mackerel are too short-lived to robustly apply these crossdating techniques given that individuals

179 lacked the overlap to crossmatch among one another. Therefore, some unknown dating error

180 remains. The biennial pattern of wide and narrow increments observed across many individuals

181 may have helped reduce some of this dating error, as it was often used to resolve decisions

182 regarding growth observed at the otolith edge (i.e., whether edge growth should be attributed to

183 the year of collection or the previous calendar year).

184

185 *2.3 Biochronology development (mixed modeling)*

186 Linear mixed models were used to assess various potential predictors of otolith growth,

187 similar to methods described in Morrongiello and Thresher (2015) and Matta et al. (2018).

188 Otolith increment widths are generally an allometric function of age at formation (Helser et al.,

189 2012), such that otolith growth can be modeled as

190

$$W_{ij} = a_j A_{ij}^{b_j},$$

192

193 where W is the width of the ith increment formed at age A of the jth fish. Increment width and

194 increment age were natural log-transformed to linearize the data and stabilize the variance

195 structure, such that $y_{ij} = \ln(W_{ij})$, $\alpha_j = \ln(a_j)$, $\beta_j = b_j$, and $x_{ij} = \ln(A_{ij})$. Models with random intercepts

196 and age slopes for each specimen were considered to allow each fish to have its own growth

197   trajectory. These models were extended to consider potential effects of sex and age at capture

198   (intrinsic fixed factors), calendar year of formation and cohort (random factors), and finally,

199   effects of both environmental and biological extrinsic fixed factors (Morrongiello and Thresher,

200   2015; Matta et al., 2018). The most complex possible model took the form:

201

202     $$y_{ijkl} = (\bar{\alpha} + \alpha_i^S + \alpha_k^Y + \alpha_l^C) + (\bar{\beta} + \beta_{ij}^S + \beta_{jk}^Y + \beta_{jl}^C)x_{ijkl} + f(\cdot) + \varepsilon_{ijkl} \, ,$$

203

204   where y_{ijkl} is the width of the annual growth increment relative the age at formation (x_{ijkl}) for fish

205   i at age j in year k and cohort l, $\bar{\alpha}$ and $\bar{\beta}$ are the fixed mean intercept and slope that describe the

206   population-wide decline in increment width as a function of age, α_i^S and β_{ij}^S are random effects

207   describing the growth trajectories of individual specimens with respect to age, α_k^Y and β_{jk}^Y are the

208   random year intercept and the corresponding slope with respect to age, α_l^C and β_{jl}^C are the

209   random cohort intercept and the corresponding slope with respect to age, and $f(\cdot)$ represents

210   additional fixed factors, (e.g., intrinsic factors sex and age at capture, and extrinsic factors

211   described in detail in Section 2.4). Continuous variables were mean-centered prior to model

212   fitting to aid convergence. A compound symmetry covariance structure was assumed (i.e., all

213   variances were considered homogenous). Relationships between extrinsic fixed effects were

214   examined for collinearity using pairwise plots, correlation coefficients, and variance inflation

215   factors (Zuur et al., 2009).

216   Models were fitted using the *lme4* package (Bates et al., 2015b) in R statistical computing

217   software (R Core Team, 2019). First, restricted maximum likelihood (REML) was used to fit

218   models to identify the optimal structure of the random components (specimen, cohort, and year).

219   This was accomplished using the maximal intrinsic fixed effect parameterization of age * sex +

220   age at capture (Morrongiello and Thresher, 2015). Models were considered that allowed the

221   random effects to vary with age. Models with various random effects structures were assessed

222   for singularity, an indication of possible over-parameterization, using the isSingular() function in

223   R statistical computing software (R Core Team, 2019). We also performed a principal

224   components analysis of the random effects structure (rePCA function) to determine the

225   proportion of variance explained by each random effect, eliminating any random slopes that were

226   not supported by the data (Bates et al., 2015a). Next, maximum likelihood (ML) was used to fit

227   models to identify the optimal structure of the intrinsic fixed components. Finally, the model

228   with the optimal random and fixed intrinsic structure was extended to add extrinsic fixed factors

229   (see Section 2.4). The most parsimonious model was refitted to the data using REML to provide

230   unbiased parameter estimates (Zuur et al., 2009). Model selection was based on Akaike's

231   Information Criterion corrected for small sample sizes (AIC_c) (Burnham and Anderson, 2002).

232   Models were ranked by AIC_c differences, or $\Delta_i = AIC_{ci} - AIC_{cmin}$, where AIC_{ci} is the AIC_c of the

233   ith model and AIC_{cmin} is the minimum AIC_c value of the models compared. The model with $\Delta_i =$

234   0 is considered the most parsimonious, and models with $\Delta_i > 10$ have essentially no support

235   (Burnham and Anderson, 2002). We also calculated the Akaike weight (AIC_{wt}), a measure of the

236   relative likelihood (probability ranging from 0 to 1) of the model given the data (Burnham and

237   Anderson, 2002). Finally, for each model we calculated the marginal R^2 (R_m^2) and the conditional

238   R^2 (R_c^2), which explain the proportion of the variance explained by the fixed factors alone and the

239   fixed and random factors combined, respectively (Nakagawa and Schielzeth, 2013).

240   Prior to the addition of extrinsic fixed factors, the random year effects from the most

241   parsimonious model were extracted. The year intercepts encapsulate all random environmental

242   variation after age-related declines in growth and other intrinsic factors have been accounted for,

243 and can be considered analogous to the "master chronology" produced by the regional curve

244 standardization technique used in dendrochronology (Helser et al., 2012). The random year

245 intercepts are reported here for comparison with previously published biochronologies, and with

246 time series that were too short to explicitly include in our mixed effects models (indices of body

247 condition and zooplankton abundance; see Section 2.4).

248

249 *2.4 Environmental and biological datasets*

250 Extrinsic oceanographic and biological factors hypothesized to have effects on otolith

251 growth were considered in the linear mixed effects models described in Section 2.3. With respect

252 to climate variables, gridded Hadley ISST 1° monthly sea surface temperatures (Rayner, 2003)

253 were obtained from the KNMI Climate Explorer (http://climexp.knmi.nl, retrieved 12/3/2018) and

254 averaged over the area 51-53°N, 172-174°W to calculate a regional mean-annual temperature

255 specific to Seguam Pass. Due to strong vertical mixing, sea surface temperature likely represents

256 relative interannual variation in water temperature throughout the water column (Stabeno et al.,

257 2005). Annual temperatures were used recognizing that otolith growth, while peaking in the

258 summer and minimized in the winter, occurs over a large portion of the year and actual timing of

259 deposition may differ at different life stages or on an individual basis (Kimura et al., 2007).

260 However, we noted that annual mean temperatures were well-correlated with seasonal mean

261 temperatures across the years 1980-2017, with Pearson correlation coefficients ranging from

262 0.62 in winter to 0.89 in summer. Therefore, annual mean temperatures likely well represent

263 overall interannual variability in water temperatures at Seguam Pass.

264 We also included an index of pink salmon abundance (Irvine and Ruggerone, 2016). Pink

265 salmon, which due to their semelparous 2-year spawning cycle are typically far more abundant in

266 odd years in the North Pacific (Ruggerone et al., 2010), are also significant predators of

267 zooplankton (Davis et al., 2005; Karpenko et al., 2007). The large Eastern Kamchatka population

268 of pink salmon, which occupies the Central and Eastern Aleutians during its ocean-going phase,

269 is known to induce trophic cascades (Batten et al., 2018) and compete with other species for

270 resources (Ruggerone and Nielsen, 2004; Springer and van Vliet, 2014). Finally, we included

271 estimates of age-3+ biomass (ln-transformed) from the Aleutian Islands Atka mackerel stock

272 assessment (Lowe et al., 2017) to account for any density-dependent, intraspecific competition

273 between adult fish that may affect growth.

274   While we wanted to include additional variables such as prey abundance explicitly in the

275 mixed effects models, those time series were not sufficiently long. Including them would require

276 truncating the growth increment data and result in lost information with respect to other

277 explanatory variables. However, these indices can still be compared against the random year

278 intercepts from the most parsimonious intrinsic model (i.e., the otolith biochronology, see

279 Section 2.3) for informational purposes. Pearson correlation coefficients were calculated between

280 the otolith biochronology and annual means of each of the following biological metrics.

281   Zooplankton comprise a significant portion of the Atka mackerel diet. Therefore we

282 compared indices of copepod and euphausiid abundance with the otolith biochronology.

283 Abundance estimates (number per sample) of copepods and euphausiids were obtained from

284 Continuous Plankton Recorder (CPR) tows (Batten et al., 2003; Batten et al., 2018). Copepods

285 were separated into "large" (> 2 mm) and "small" (< 2 mm) categories with the understanding

286 that the two size groups may occupy different roles in terms of trophic energy transfer (Mazur et

287 al., 2007). The CPR data were collected continuously around the clock from 2000-2014 in the

288 Southern Bering Sea closest in proximity to the study area, the same region in which the Eastern

289   Kamchatka population of pink salmon has been shown to impact plankton communities (Batten

290   et al., 2018). Connectivity between this region and Seguam Pass has been demonstrated by

291   Stabeno et al. (2005); strong tidal currents within and adjacent to Seguam Pass flow north,

292   providing an important source of nutrients to the Southern Bering Sea. Data were averaged

293   across multiple tows during the summer months (June-August) for each year of collection to

294   estimate the mean abundance of each zooplankton category. Only summer data were used

295   because they allowed for the best time series continuity of the CPR sampling dataset and to

296   maintain consistency with Batten et al. (2018). Further details regarding CPR sampling and

297   analysis are described in Batten et al. (2003).

298   The otolith biochronology was also compared to fish body condition outside of the mixed

299   effects models. This metric was based on length and weight observations from 13,013 fish

300   collected by observers aboard commercial fishery vessels in NMFS Statistical Area 541 from

301   1990-2015. We calculated the relative condition factor K_n (Blackwell et al., 2000), where K_n is

302   the weight of an individual fish divided by the length-specific mean weight. (Length-specific

303   mean weight was calculated separately for each sex and month of collection, to control for

304   potential sex-specific differences and seasonal variation related to reproduction.) Therefore, a

305   fish in average condition for its length/sex/month category would have a K_n of 1, and those

306   above or below average condition would have a K_n of > 1 or < 1, respectively. All K_n values

307   were then averaged by year to generate a relative annual index of condition representative of the

308   population at Seguam Pass for comparison with the otolith biochronology.

309

310

3. Results

Otoliths from 409 Atka mackerel collected between 1996 and 2015 were examined during this study. Of these, 289 fish (71%) had increment boundaries that were deemed sufficiently clear for measurement (Table 1, Fig. 2). There were 172 females and 117 males in the otolith measurement sample, and fish ranged from 5 to 12 years in age at capture. A total of 1,426 growth increments were measured, producing a 28-year biochronology spanning 1988-2015.

In our model selection process (based on Δ_i), the model with the optimal random effects structure included a random intercept and slope for each specimen with respect to age at increment formation, thereby allowing each specimen to have its own growth trajectory, as well as random year and cohort intercepts. Of the possible combinations of intrinsic fixed effects, only age at increment formation and age at capture were found to contribute to variation in growth (sex was not a factor in the most parsimonious model). We then extended the optimal intrinsic model to include the extrinsic fixed effects of Atka mackerel abundance, pink salmon abundance, and water temperature. None of the correlation coefficients between extrinsic fixed effects were significant, and variance inflation factors were all below 2.0, indicating there was no collinearity among these explanatory variables (Zuur et al., 2007).

The most parsimonious full model ($\Delta_i = 0$) included an effect of pink salmon abundance on variation in growth of Atka mackerel growth increments (Table 2; Table A.1). The Δ_i of the next best model, which included terms for temperature and pink salmon abundance, indicated some support; however, comparison of the AIC_{wt} of the two models suggested the pink salmon abundance-only model was ~2.5 times more likely to be the model best representing the data

334   (Wagenmakers and Farrell, 2004). The other candidate extrinsic models had little to no support

335   based on Δ_i and AIC_{wt}, indicating low probability for effects of temperature or Atka mackerel

336   abundance on variability in otolith growth (Table A.1).

337   In the best intrinsic model (not including effects of pink salmon abundance), the otolith

338   biochronology was characterized by a biennial pattern of lower than average growth in odd years

339   followed by higher than average growth in even years, with an overall upward trend during the

340   most recent decade (Fig. 3a). Additionally, growth varied by cohort, with some cohorts

341   outperforming others; this relationship also appeared somewhat cyclical albeit on a longer

342   timeframe than the year effect (Fig. 3b). The magnitude of the year effect was greater than that

343   of the cohort effect.

344   In the full model (including all intrinsic and extrinsic effects), we observed an age-related

345   decline in growth-increment width (Fig. 4a). We also observed a very slight increase in growth

346   with respect to the age the fish was at the time of its capture (Fig. 4b), indicating that fish that

347   were older at capture were generally faster growers than those that were younger at capture.

348   Finally, we observed a negative relationship between otolith growth of Atka mackerel and

349   abundance of Eastern Kamchatka pink salmon (Fig. 4c). The full model explained a high

350   proportion of the total variance in otolith growth ($R^2_c = 0.806$). The R^2_m value of this model

351   (0.694), the proportion of the variance explained by fixed factors only, indicated that inclusion of

352   pink salmon abundance explained slightly more of the variance than the intrinsic model (0.680).

353   The otolith biochronology (the random year intercepts from the best intrinsic model) was

354   significantly correlated with several biological indices (Table 3). The otolith biochronology was

355   significantly and positively related to abundance of large copepods in the Southern Bering Sea (r

356     $= 0.58, p = 0.023$). This relationship was strongest over the years 2000-2010, with a correlation

357   coefficient of 0.87 ($p < 0.001$). However, after 2011 this relationship became somewhat

358   uncoupled, particularly in the year 2013 where the two time series varied inversely (Fig. 5a). The

359   otolith biochronology was negatively related to abundance of small copepods (Fig. 5b) and

360   abundance of pink salmon (Fig. 5c). The relationship between the otolith biochronology and pink

361   salmon abundance was strongest between the years 1990 and 2010 ($r = -0.74$, $p < 0.001$), and

362   similar to the relationship with large copepods, the relationship between the otolith

363   biochronology and pink salmon became uncoupled in 2013 due the anomalously low abundance

364   of pink salmon in that year. The otolith biochronology was not significantly related with

365   euphausiid abundance (Table 3). There was no significant relationship between the Atka

366   mackerel biochronology and body condition, or between body condition and any of the other

367   biological time series (Table 3).

368

369

370   **4. Discussion**

371

372   In this study, we generated a 28-year otolith biochronology for Atka mackerel, one of the

373   most abundant groundfish species in the Aleutian Islands, Alaska. To the best of our knowledge,

374   this is the first published biochronology from this important large marine ecosystem, as well as

375   one of the first biochronologies anywhere to highlight the importance of upper-trophic level

376   processes relative to otolith growth. This work suggests that biotic interactions are among the

377   most important extrinsic controls on growth of Atka mackerel at Seguam Pass in the Aleutian

378   Islands ecosystem. In particular, we found evidence of competition between pink salmon and

379   Atka mackerel for shared food resources. Both species are zooplanktivores and forage within the

380   top 50 m of the water column (Nichol and Somerton, 2002; Armstrong et al., 2005), with

381   calanoid copepods and euphausiids comprising a major part of their diets (Yang, 1999; Davis et

382   al., 2005; Karpenko et al., 2007; Armstrong et al., 2008; Rand et al., 2010).

383   Pink salmon is the dominant salmonid species in the North Pacific and is biennially

384   highly abundant (Ruggerone and Irvine, 2018). Pink salmon are voracious predators in the North

385   Pacific Ocean, impacting food webs through predation and competition, particularly the large

386   Eastern Kamchatka population, the range of which extends to 155ºW during its ocean-going

387   phase (Ruggerone and Nielsen, 2004; Springer and van Vliet, 2014). During odd years when

388   they are highly abundant, pink salmon have been shown to depress populations of large

389   copepods, which in turn reduces grazing pressure on phytoplankton, allowing them to flourish

390   (Shiomoto et al., 1997; Kobari et al., 2003; Batten et al., 2018). Also during these odd years

391   when they are abundant, pink salmon have been shown to outcompete other North Pacific marine

392   predators for shared resources, reducing growth and survival of sockeye (*O. nerka*), chum (*O.*

393   *keta*), and Chinook salmon (*O. tshawytscha*) (Ruggerone et al., 2003; Ruggerone and Nielsen,

394   2004) and even altering hatch dates and reducing growth and breeding success in seabirds

395   (Springer and van Vliet, 2014). There is also evidence of competition between juvenile

396   groundfishes and pink salmon in the eastern Gulf of Alaska in years when resources are limited

397   (Daly et al., 2019).

398   Copepods in general dominate the zooplankton biomass in the Aleutian Islands (Zador

399   and Ortiz, 2018) and are an important component of the Atka mackerel diet. Indeed, we observed

400   a strong positive relationship between the abundance of large copepods and otolith growth.

401   However, there was some temporal variation in the strength of this relationship. The relative

402   abundance of pink salmon, as predicted by its 2-year life cycle and tendency to be highly

403   abundant in odd years, was unexpectedly low in 2013 and high in 2014, resulting in cascading

404   effects on zoo- and phytoplankton communities (Batten et al., 2018). During this same

405   timeframe, the relationships among the otolith biochronology, large copepods, and pink salmon

406   broke down, which could indicate additional unexplained effects on growth, or possible temporal

407   flexibility in the Atka mackerel diet at the study location. For example, in the northern portion of

408   Seguam Pass, fish have also been found to be an important component of the diet of Atka

409   mackerel, especially compared to the western Aleutian Islands (Rand et al., 2010). Still, the

410   overall relationships observed among the otolith biochronology, pink salmon index, and large

411   copepod index suggest the potential for competition between the two fish predators over this

412   important, energetically-rich prey resource. We hypothesize that in years when pink salmon

413   abundance is high, they overgraze large copepods, resulting in lower availability for Atka

414   mackerel, thereby reducing the capacity for growth. In years when pink salmon abundance is

415   low, Atka mackerel are able to capitalize on this food resource and experience overall higher

416   growth. To the best of our knowledge, direct impacts of pink salmon have not been described for

417   other groundfish species in the Aleutian Islands. Given our findings, such potential effects may

418   be worthy of further exploration.

419   Interestingly, the Atka mackerel otolith biochronology had a negative relationship with

420   abundance of small copepods, and no relationship with euphausiid abundance, despite

421   euphausiids being another significant part of the Atka mackerel diet (Yang, 1999, 2003). Though

422   the CPR is known to under-sample large euphausiids (Batten et al., 2018), the rate is assumed to

423   be consistent, and thus should capture relative year-to-year changes in abundance (S. Batten,

424   pers. comm., Marine Biological Association UK, Nanaimo, British Columbia, Canada). The

425   observed relationships between zooplankton abundance and the otolith biochronology may be a

426 result of the spatial distribution of zooplankton prey fields with respect to our sample collection

427 locations. Most of our specimens were collected in the southern portion of Seguam Pass, where

428 large oceanic copepods dominate the zooplankton community (Coyle, 2005). It could be,

429 therefore, within that small region of Seguam Pass, that large copepods are the main limiting

430 resource to Atka mackerel growth. Or, there may be additional unknown sources contributing to

431 variation in growth. Further studies of spatial and temporal variation in Atka mackerel diet

432 preferences may clarify some of these issues. Also worthy of further investigation are the

433 processes driving the observed relationships between the otolith biochronology and abundance of

434 large and small copepods. Detailed examination of copepod size spectra within Atka mackerel

435 diets could elucidate whether the observed biennial patterns are consistent with the relative size

436 composition of copepod prey consumed in odd and even years.

437 Unlike other previous otolith biochronology studies in the adjacent eastern Bering Sea

438 (Matta et al., 2010; van der Sleen et al., 2016) and Gulf of Alaska (von Biela et al., 2015; Matta

439 et al., 2018), temperature was not a predictor of growth. The Aleutian Islands are a unique

440 ecosystem with very different oceanographic and biological dynamics than the Bering Sea and

441 Gulf of Alaska. Seguam Pass in particular is characterized by strong currents and top-to-bottom

442 vertical mixing, resulting in little stratification (Ladd et al., 2005; Stabeno et al., 2005). This in

443 turn results in relatively stable water temperatures experienced by Atka mackerel at Seguam Pass

444 from year-to-year (Rand et al., 2010, 2019). Indeed, temperature has not been found to be a

445 significant predictor of Atka mackerel density (catch per unit effort) in the Aleutian Islands

446 (Rand et al., 2019). Additionally, bioenergetic modeling has demonstrated that diet composition

447 explains far more variation in body growth in Atka mackerel than thermal experience, even

448 across a longitudinal gradient where growth varies considerably (Lowe et al., 1998; Rand et al.,

449   2010). One other possibility is that Atka mackerel may not be as sensitive to fluctuations in

450   temperature as other Alaskan groundfish. Their small (< 50 km) home ranges (McDermott et al.,

451   2005, 2016) suggest that their thermal tolerance may be relatively high, as staying in place could

452   theoretically expose them to greater temperature variability than would migrating to remain in

453   thermally uniform water masses. That, coupled with the relative stability of interannual mean

454   temperature in Seguam Pass, may explain the lack of relationship between Atka mackerel growth

455   and temperature.

456   Otolith biochronology studies often assume but rarely test the relationship between

457   otolith and somatic growth (Black et al., 2013). Here, we did not detect a significant correlation

458   between the biochronology and body condition. One possible explanation is that body condition

459   in the form we used is a measure of cumulative growth that is dependent on weight and length

460   integrated over a fish's lifetime, and therefore is inherently subject to autocorrelation. In contrast,

461   the otolith biochronology represents the relative population-wide deviation in growth for any

462   given year. Furthermore, fish weight is a far more labile trait compared to either fish length or

463   otolith size, and therefore environmentally-driven changes in condition may occur on different

464   timescales than would be captured by the otolith biochronology, making a relationship more

465   difficult to detect. Another possibility is simply that the otolith biochronology is not a perfect

466   proxy for somatic growth. However, we failed to detect any significant relationships between

467   body condition and prey abundance, suggesting that other measures of fish health and fitness

468   should be explored. There is currently no available published information regarding whether K_n

469   is actually an appropriate indicator of growth and fitness in Atka mackerel. In general, there is

470   little agreement in the literature about the best way to assess fish body condition. While more

471   direct measures such as energy density are preferred, these are typically destructive, expensive,

472   and time-consuming. Methods based on length and weight are far more common, as these data

473   can be collected cheaply and rapidly and allow for the development of long-term datasets.

474   However, one drawback of these methods is they can change seasonally and based on life history

475   and reproductive state, and some may not reflect actual body composition (Wuenschel et al.,

476   2019) or relative fitness or survival (Cox et al., 2015). These methods suffer further from

477   difficulties in standardization and thus may induce biases in body condition estimates (Blackwell

478   et al., 2000; Wuenschel et al., 2019). Clearly, further work is necessary to determine the best

479   method of assessing body condition in Atka mackerel as well as other Alaska groundfish species.

480   Most frequently, biochronology studies have been focused on long-lived fish, corals, and

481   molluscs (Black et al., 2005; Carilli et al., 2010; Peharda et al., 2016), but this method has also

482   been successfully applied to fishes with life spans similar in length to Atka mackerel

483   (Morrongiello et al., 2011; von Biela et al., 2015; van der Sleen et al., 2018). One drawback of

484   applying this approach to organisms with lower longevity is that the short lengths of the

485   individual growth time series used to build the biochronology preclude crossdating. The inability

486   to crossdate may therefore result in an unknown error rate that could mute environmental signals

487   (Black et al., 2016). Yet, a consistent alternating pattern of narrow and wide growth increments

488   was apparent in many individuals in our study, which likely reduced dating error by allowing for

489   crossmatching between clear individuals and those with potential interpretative differences with

490   respect to growth on the otolith edge. Moreover, dating errors in long-lived individuals induce

491   frame-shifts that increasingly diminish environmental signals back through time (Black et al.,

492   2016). For the Atka mackerel biochronology, any error rate, which cannot be quantified in the

493   absence of crossdating, should be constant over the length of the biochronology. A second

494   limitation inherent to biochronology studies is that precise measurements can only be taken from

495   clear specimens. However, Atka mackerel consistently have otolith patterns that are relatively

496   easy to interpret and precision among readers is high (Anderl, 2012), likely reducing the

497   potential for measurement and dating errors as well as sample-selection bias.

498   Using an otolith biochronology approach, we found evidence suggesting that growth of

499   Atka mackerel is driven by external biological factors. This study is the first of its kind located in

500   the Aleutian Islands region, to date a relatively poorly studied but large, diverse, and ecologically

501   rich marine ecosystem in the North Pacific Ocean. While previous biochronology studies in

502   Alaska waters have detected significant positive relationships between growth and temperature

503   for a variety of species including flatfish, rockfish, and greenlings (Matta et al., 2010; von Biela

504   et al., 2015; van der Sleen et al., 2016), this is the first to suggest direct linkages with biological

505   drivers, namely prey dynamics and interspecies competition. Future monitoring of these effects

506   on Atka mackerel growth within this dynamic ecosystem is warranted to determine whether

507   these interspecies relationships are truly stationary, especially given projected climate change

508   that may impact zooplankton and salmon populations.

509

510

528

References

Anderl, D.M., 2012. Atka mackerel (*Pleurogrammus monopterygius*), in: Matta, M.E., Kimura, D.K. (Eds.), Age determination manual of the Alaska Fisheries Science Center Age and Growth Program. U.S. Department of Commerce, NOAA Professional Paper 13, pp. 31-36.

Anderl, D.M., Nishimura, A., Lowe, S.A., 1996. Is the first annulus on the otolith of the Atka mackerel, *Pleurogrammus monopherygius*, missing? Fishery Bulletin, U.S. 94, 163-169.

Armstrong, J.L., Boldt, J.L., Cross, A.D., Moss, J.H., Davis, N.D., Myers, K.W., Walker, R.V., Beauchamp, D.A., Haldorson, L.J., 2005. Distribution, size, and interannual, seasonal and diel food habits of northern Gulf of Alaska juvenile pink salmon, *Oncorhynchus gorbuscha*. Deep-Sea Research Part II: Topical Studies in Oceanography 52, 247-265. https://doi.org/10.1016/j.dsr2.2004.09.019

Armstrong, J.L., Myers, K.W., Beauchamp, D.A., Davis, N.D., Walker, R.V., Boldt, J.L., Piccolo, J.J., Haldorson, L.J., Moss, J.H., 2008. Interannual and spatial feeding patterns of hatchery and wild juvenile pink salmon in the Gulf of Alaska in years of low and high survival. Transactions of the American Fisheries Society 137, 1299-1316. https://doi.org/10.1577/T07-196.1

Barrow, J., Ford, J., Day, R., Morrongiello, J., 2018. Environmental drivers of growth and predicted effects of climate change on a commercially important fish. Marine Ecology Progress Series 598, 201-212. https://doi.org/10.3354/meps12234

Bates, D.M., Kliegl, R., Vasishth, S., Baayen, H., 2015a. Parsimonious mixed models. Available at https://arxiv.org/abs/1506.04967

550   Bates, D., Maechler, M., Bolker, B., Walker, S., 2015b. Fitting linear mixed-effects models

551   using lme4. Journal of Statistical Software 67(1), 1-48. https://doi.org/10.18637/jss.v067.i01

552   Batten, S.D., Clark, R., Flinkman, J., Hays, G.C., John, E., John, A.W.G., Jonas, T., Lindley,

553   J.A., Stevens, D.P., Walne, A., 2003. CPR sampling: the technical background, materials and

554   methods, consistency and comparability. Progress in Oceanography 58, 193-215.

555   https://doi.org/10.1016/j.pocean.2003.08.004

556   Batten, S.D., Ruggerone, G.T., Ortiz, I., 2018. Pink salmon induce a trophic cascade in plankton

557   populations in the southern Bering Sea and around the Aleutian Islands. Fisheries Oceanography

558   27, 548-559. https://doi.org/10.1111/fog.12276

559   Black, B.A., Andersson, C., Butler, P.G., Carroll, M.L., DeLong, K.L., Reynolds, D.J., Schone,

560   B.R., Scourse, J., van der Sleen, P., Wanamaker, A.D., Witbaard, R., 2019. The revolution of

561   crossdating in marine palaeoecology and palaeoclimatology. Biology Letters 15, 20180665.

562   https://doi.org/10.1098/rsbl.2018.0665

563   Black, B.A., Boehlert, G.W., Yoklavich, M.M., 2005. Using tree-ring crossdating techniques to

564   validate annual growth increments in long-lived fishes. Canadian Journal of Fisheries and

565   Aquatic Sciences 62, 2277-2284. https://doi.org/10.1139/f05-142

566   Black, B.A., Boehlert, G.W., Yoklavich, M.M., 2008. Establishing climate-growth relationships

567   for yelloweye rockfish (*Sebastes ruberrimus*) in the northeast Pacific using a

568   dendrochronological approach. Fisheries Oceanography 17, 368-379.

569   https://doi.org/10.1111/j.1365-2419.2008.00484.x

570 Black, B.A., Griffin, D., van der Sleen, P., Wanamaker, A.D., Jr., Speer, J.H., Frank, D.C.,

571 Stahle, D.W., Pederson, N., Copenheaver, C.A., Trouet, V., Griffin, S., Gillanders, B.M., 2016.

572 The value of crossdating to retain high-frequency variability, climate signals, and extreme events

573 in environmental proxies. Global Change Biology 22, 2582-2595.

574 https://doi.org/10.1111/gcb.13256

575 Black, B.A., Matta, M.E., Helser, T.E., Wilderbuer, T.K., 2013. Otolith biochronologies as

576 multidecadal indicators of body size anomalies in yellowfin sole (*Limanda aspera*). Fisheries

577 Oceanography 22, 523-532. https://doi.org/10.1111/fog.12036

578 Black, B.A., Schroeder, I.D., Sydeman, W.J., Bograd, S.J., Wells, B.K., Schwing, F.B., 2011.

579 Winter and summer upwelling modes and their biological importance in the California Current

580 Ecosystem. Global Change Biology 17, 2536-2545. https://doi.org/10.1111/j.1365-

581 2486.2011.02422.x

582 Blackwell, B.G., Brown, M.L., Willis, D.W., 2000. Relative weight (Wr) status and current use

583 in fisheries assessment and management. Reviews in Fisheries Science 8, 1-44.

584 https://doi.org/10.1080/10641260091129161

585 Burnham, K.P., Anderson, D.R., 2002. Model selection and multimodel inference: a practical

586 information-theoretic approach, 2nd ed. Springer, New York.

587 Carilli, J.E., Norris, R.D., Black, B., Walsh, S.M., McField, M., 2010. Century-scale records of

588 coral growth rates indicate that local stressors reduce coral thermal tolerance threshold. Global

589 Change Biology 16, 1247-1257. https://doi.org/10.1111/j.1365-2486.2009.02043.x

590   Cooper, D.W., McDermott, S.F., Ianelli, J.N., 2010. Spatial and temporal variability in Atka

591   mackerel female maturity at length and age. Marine and Coastal Fisheries 2, 329-338.

592   https://doi.org/10.1577/C09-045.1

593   Cox, R.M., Calsbeek, R., Blanckenhorn, W., 2015. Survival of the fattest? Indices of body

594   condition do not predict viability in the brown anole (*Anolis sagrei*). Functional Ecology 29,

595   404-413. https://doi.org/10.1111/1365-2435.12346

596   Coyle, K.O., 2005. Zooplankton distribution, abundance and biomass relative to water masses in

597   eastern and central Aleutian Island passes. Fisheries Oceanography 14, 77-92.

598   https://doi.org/10.1111/j.1365-2419.2005.00367.x

599   Daly, E.A., Moss, J.H., Fergusson, E., Brodeur, R.D., 2019. Potential for resource competition

600   between juvenile groundfishes and salmon in the eastern Gulf of Alaska. Deep-Sea Research Part

601   II: Topical Studies in Oceanography. https://doi.org/10.1016/j.dsr2.2019.06.007

602   Davis, N.D., Fukuwaka, M., Armstrong, J.L., Myers, K.W., 2005. Salmon food habits studies in

603   the Bering Sea, 1960 to present. NPAFC Technical Report 6, pp. 24-28.

604   Doubleday, Z.A., Izzo, C., Haddy, J.A., Lyle, J.M., Ye, Q., Gillanders, B.M., 2015. Long-term

605   patterns in estuarine fish growth across two climatically divergent regions. Oecologia 179, 1079-

606   1090. https://doi.org/10.1007/s00442-015-3411-6

607   Douglass, A.E., 1920. Evidence of climatic effects in the annual rings of trees. Ecology 1, 24-32.

608   https://doi.org/10.2307/1929253

609   Helser, T.E., Lai, H.L., Black, B.A., 2012. Bayesian hierarchical modeling of Pacific geoduck

610   growth increment data and climate indices. Ecological Modelling 247, 210-220.

611   https://doi.org/10.1016/j.ecolmodel.2012.08.024

612   Irvine, J.R., Ruggerone, G.T., 2016. Provisional estimates of numbers and biomass for natural-

613   origin and hatchery-origin pink, chum, and sockeye salmon in the North Pacific, 1952-2015.

614   NPAFC Doc. 1660. Fisheries and Oceans Canada, Pacific Biological Station and Natural

615   Resources Consultants, Inc, 45 pp.

616   Karpenko, V.I., Volkov, A.F., Koval, M.V., 2007. Diets of Pacific salmon in the Sea of Okhotsk,

617   Bering Sea, and Northwest Pacific Ocean. North Pacific Anadramous Fish Commission Bulletin

618   4, 105-116.

619   Kimura, D.K., Anderl, D.M., Goetz, B.J., 2007. Seasonal marginal growth on otoliths of seven

620   Alaska groundfish species support the existence of annual patterns. Alaska Fishery Research

621   Bulletin 12, 243-251.

622   Kobari, T., Ikeda, T., Kanno, Y., Shiga, N., Takagi, S., Azumaya, T., 2003. Interannual

623   variations in abundance and body size in *Neocalanus* copepods in the central North Pacific.

624   Journal of Plankton Research 25, 483-494. https://doi.org/10.1093/plankt/25.5.483

625   Ladd, C., Hunt, G.L., Mordy, C.W., Salo, S.A., Stabeno, P.J., 2005. Marine environment of the

626   eastern and central Aleutian Islands. Fisheries Oceanography 14, 22-38.

627   https://doi.org/10.1111/j.1365-2419.2005.00373.x

628   Lauth, R.R., Guthridge, J., Nichol, D.G., McEntire, S.W., Hillgruber, N., 2007a. Timing and

629   duration of mating and brooding periods of Atka mackerel (*Pleurogrammus monopterygius*) in

630   the North Pacific Ocean. Fishery Bulletin, U.S. 105, 560-570.

631   Lauth, R.R., McEntire, S.W., Zenger, H.H., 2007b. Geographic distribution, depth range, and

632   description of Atka mackerel *Pleurogrammus monopterygius* nesting habitat in Alaska. Alaska

633   Fishery Research Bulletin 12, 165-186.

634   Lorenzen, K., 2016. Toward a new paradigm for growth modeling in fisheries stock assessments:

635   Embracing plasticity and its consequences. Fisheries Research 180, 4-22.

636   https://doi.org/10.1016/j.fishres.2016.01.006

637   Lowe, S., Ianelli, J., Palsson, W., 2017. Assessment of the Atka mackerel stock in the Bering Sea

638   and Aleutian Islands. In: Stock assessment and fishery evaluation report for the groundfish

639   resources of the Bering Sea/Aleutian Islands regions. North Pacific Fishery Management

640   Council, 605 West 4th, Suite 306, Anchorage, Alaska 99501-2252.

641   Lowe, S.A., Van Doornik, D.M., Winans, G.A., 1998. Geographic variation in genetic and

642   growth patterns of Atka mackerel, *Pleurogrammus monopterygius* (Hexagrammidae), in the

643   Aleutian archipelago. Fishery Bulletin, U.S. 96, 502-515.

644   Matta, M.E., Black, B.A., Wilderbuer, T.K., 2010. Climate-driven synchrony in otolith growth-

645   increment chronologies for three Bering Sea flatfish species. Marine Ecology Progress Series

646   413, 137-145. https://doi.org/10.3354/meps08689

647   Matta, M.E., Helser, T.E., Black, B.A., 2018. Intrinsic and environmental drivers of growth in an

648   Alaskan rockfish: an otolith biochronology approach. Environmental Biology of Fishes 101,

649   1571-1587. https://doi.org/10.1007/s10641-018-0801-8

650   Mazur, M.M., Wilson, M.T., Dougherty, A.B., Buchheister, A., Beauchamp, D.A., 2007.

651   Temperature and prey quality effects on growth of juvenile walleye pollock *Theragra*

652   *chalcogramma* (Pallas): a spatially explicit bioenergetics approach. Journal of Fish Biology 70,

653   816-836. https://doi.org/10.1111/j.1095-8649.2007.01344.x

654   McDermott, S.F., Fritz, L.W., Haist, V., 2005. Estimating movement and abundance of Atka

655   mackerel (*Pleurogrammus monopterygius*) with tag–release–recapture data. Fisheries

656   Oceanography 14, 113-130. https://doi.org/10.1111/j.1365-2419.2005.00380.x

657   McDermott, S.F., Haist, V., Rand, K.M., 2016. Evaluating the efficacy of trawl exclusion zones

658   by estimating local Atka mackerel abundance and movement patterns in the central and eastern

659   Aleutian Islands. Marine and Coastal Fisheries 8, 334-349.

660   https://doi.org/10.1080/19425120.2015.1135218

661   McDermott, S.F., Lowe, S.A., 1997. The reproductive cycle and sexual maturity of Atka

662   mackerel, *Pleurogrammus monopterygius*, in Alaska waters. Fishery Bulletin, U.S. 95, 321-333.

663   Morais, R.A., Bellwood, D.R., 2018. Global drivers of reef fish growth. Fish and Fisheries 19,

664   874-889. https://doi.org/10.1111/faf.12297

665   Mordy, C.W., Stabeno, P.J., Ladd, C., Zeeman, S., Wisegarver, D.P., Salo, S.A., Hunt, G.L.,

666   2005. Nutrients and primary production along the eastern Aleutian Island Archipelago. Fisheries

667   Oceanography 14, 55-76. https://doi.org/10.1111/j.1365-2419.2005.00364.x

668   Morrongiello, J.R., Crook, D.A., King, A.J., Ramsey, D.S.L., Brown, P., 2011. Impacts of

669   drought and predicted effects of climate change on fish growth in temperate Australian lakes.

670   Global Change Biology 17, 745-755. https://doi.org/10.1111/j.1365-2486.2010.02259.x

671   Morrongiello, J.R., Thresher, R.E., 2015. A statistical framework to explore ontogenetic growth

672   variation among individuals and populations: a marine fish example. Ecological Monographs 85,

673   93-115. https://doi.org/10.1890/13-2355.1

674   Morrongiello, J.R., Thresher, R.E., Smith, D.C., 2012. Aquatic biochronologies and climate

675   change. Nature Climate Change 2, 849-857. https://doi.org/10.1038/nclimate1616

676   Nakagawa, S., Schielzeth, H., 2013. A general and simple method for obtaining R^2 from

677   generalized linear mixed-effects models. Methods in Ecology and Evolution 4, 133-142.

678   https://doi.org/10.1111/j.2041-210x.2012.00261.x

679   Nichol, D.G., Somerton, D.A., 2002. Diurnal vertical migration of the Atka mackerel

680   *Pleurogrammus monopterygius* as shown by archival tags. Marine Ecology Progress Series 239,

681   193-207. https://doi.org/10.3354/meps239193

682   Oliver, E.C.J., Burrows, M.T., Donat, M.G., Sen Gupta, A., Alexander, L.V., Perkins-

683   Kirkpatrick, S.E., Benthuysen, J.A., Hobday, A.J., Holbrook, N.J., Moore, P.J., Thomsen, M.S.,

684   Wernberg, T., Smale, D.A., 2019. Projected marine heatwaves in the 21st century and the

685   potential for ecological impact. Frontiers in Marine Science 6, 734

686   https://doi.org/10.3389/fmars.2019.00734

687   Ong, J.J.L., Rountrey, A.N., Black, B.A., Nguyen, H.M., Coulson, P.G., Newman, S.J.,

688   Wakefield, C.B., Meeuwig, J.J., Meekan, M.G., 2018. A boundary current drives synchronous

689   growth of marine fishes across tropical and temperate latitudes. Global Change Biology 24,

690   1894-1903. https://doi.org/10.1111/gcb.14083

691   O'Reilly, C.H., 2018. Interdecadal variability of the ENSO teleconnection to the wintertime

692   North Pacific. Climate Dynamics 51, 3333-3350. https://doi.org/10.1007/s00382-018-4081-y

693   Peharda, M., Black, B.A., Purroy, A., Mihanovic, H., 2016. The bivalve *Glycymeris pilosa* as a

694   multidecadal environmental archive for the Adriatic and Mediterranean Seas. Marine

695   Environmental Research 119, 79-87. https://doi.org/10.1016/j.marenvres.2016.05.022

696   R Core Team, 2019. R: A language and environment for statistical computing. R Foundation for

697   Statistical Computing, Vienna, Austria. https://www.R-project.org

698   Rand, K.M., Beauchamp, D.A., Lowe, S.A., 2010. Longitudinal growth differences and the

699   influence of diet quality on Atka mackerel of the Aleutian Islands, Alaska: using a bioenergetics

700   model to explore underlying mechanisms. Marine and Coastal Fisheries 2, 362-374.

701   https://doi.org/10.1577/C09-046.1

702   Rand, K.M., McDermott, S.F., Logerwell, E., Matta, M.E., Levine, M., Bryan, D.R., Loomis, T.,

703   2019. Higher aggregation of key prey species associated with diet and abundance of Steller sea

704   lion *Eumetopias jubatus* across the Aleutian Islands. Marine and Coastal Fisheries 11, 472-486.

705   https://doi.org/10.1002/mcf2.10096

706   Rayner, N.A., 2003. Global analyses of sea surface temperature, sea ice, and night marine air

707   temperature since the late nineteenth century. Journal of Geophysical Research 108, 4407.

708   https://doi.org/10.1029/2002JD002670

709   Ruggerone, G.T., Irvine, J.R., 2018. Numbers and biomass of natural- and hatchery-origin pink

710   salmon, chum salmon, and sockeye salmon in the North Pacific Ocean, 1925-2015. Marine and

711   Coastal Fisheries 10, 152-168. https://doi.org/10.1002/mcf2.10023

712   Ruggerone, G.T., Nielsen, J.L., 2004. Evidence for competitive dominance of pink salmon

713   (*Oncorhynchus gorbuscha*) over other salmonids in the North Pacific Ocean. Reviews in Fish

714   Biology and Fisheries 14, 371-390. https://doi.org/10.1007/s11160-004-6927-0

715   Ruggerone, G.T., Peterman, R.M., Dorner, B., Myers, K.W., 2010. Magnitude and trends in

716   abundance of hatchery and wild pink salmon, chum salmon, and sockeye salmon in the North

717   Pacific Ocean. Marine and Coastal Fisheries 2, 306-328. https://doi.org/10.1577/C09-054.1

718   Ruggerone, G.T., Zimmermann, M., Myers, K.W., Nielsen, J.L., Rogers, D.E., 2003.

719   Competition between Asian pink salmon (*Oncorhynchus gorbuscha*) and Alaskan sockeye

720   salmon (*O. nerka*) in the North Pacific Ocean. Fisheries Oceanography 12, 209-219.

721   https://doi.org/10.1046/j.1365-2419.2003.00239.x

722   Shiomoto, A., Tadokoro, K., Nagasawa, K., Ishida, Y., 1997. Trophic relations in the subarctic

723   North Pacific ecosystem: possible feeding effect from pink salmon. Marine Ecology Progress

724   Series 150, 75-85. https://doi.org/10.3354/meps150075

725   Sibly, R.M., Baker, J., Grady, J.M., Luna, S.M., Kodric-Brown, A., Venditti, C., Brown, J.H.,

726   2015. Fundamental insights into ontogenetic growth from theory and fish. Proceedings of the

727   National Academy of Sciences 112, 13934-13939. https://doi.org/10.1073/pnas.1518823112

728   Sinclair, E.H., Johnson, D.S., Zeppelin, T.K., Gelatt, T.S., 2013. Decadal variation in the diet of

729   Western Stock Steller sea lions (*Eumetopias jubatus*). U.S. Department of Commerce, NOAA

730   Technical Memorandum, NMFS-AFSC-248, 67 p.

731   Sinclair, E.H., Moore, S.E., Friday, N.A., Zeppelin, T.K., Waite, J.M., 2005. Do patterns of

732   Steller sea lion (*Eumetopias jubatus*) diet, population trend and cetacean occurrence reflect

733   oceanographic domains from the Alaska Peninsula to the central Aleutian Islands? Fisheries

734   Oceanography 14, 223-242. https://doi.org/10.1111/j.1365-2419.2005.00375.x

735   Springer, A.M., van Vliet, G.B., 2014. Climate change, pink salmon, and the nexus between

736   bottom-up and top-down forcing in the subarctic Pacific Ocean and Bering Sea. Proceedings of

737   the National Academy of Sciences USA 111(18), E1880-1888.

738   https://doi.org/10.1073/pnas.1319089111

739   Stabeno, P.J., Kachel, D.G., Kachel, N.B., Sullivan, M.E., 2005. Observations from moorings in

740   the Aleutian Passes: temperature, salinity and transport. Fisheries Oceanography 14, 39-54.

741   https://doi.org/10.1111/j.1365-2419.2005.00362.x

742   Stawitz, C.C., Essington, T.E., Branch, T.A., Haltuch, M.A., Hollowed, A.B., Spencer, P.D.,

743   2015. A state-space approach for detecting growth variation and application to North Pacific

744   groundfish. Canadian Journal of Fisheries and Aquatic Sciences 72, 1316-1328.

745   https://doi.org/10.1139/cjfas-2014-0558

746   van der Sleen, P., Dzaugis, M.P., Gentry, C., Hall, W.P., Hamilton, V., Helser, T.E., Matta,

747   M.E., Underwood, C.A., Zuercher, R., Black, B.A., 2016. Long-term Bering Sea environmental

748   variability revealed by a centennial-length biochronology of Pacific ocean perch *Sebastes alutus*.

749   Climate Research 71, 33-45. https://doi.org/10.3354/cr01425

750   van der Sleen, P., Stransky, C., Morrongiello, J.R., Haslob, H., Peharda, M., Black, B.A., 2018.

751   Otolith increments in European plaice (*Pleuronectes platessa*) reveal temperature and density-

752   dependent effects on growth. ICES Journal of Marine Science 75, 1655-1663.

753   https://doi.org/10.1093/icesjms/fsy011

754   von Biela, V.R., Kruse, G.H., Mueter, F.J., Black, B.A., Douglas, D.C., Helser, T.E.,

755   Zimmerman, C.E., 2015. Evidence of bottom-up limitations in nearshore marine systems based

756   on otolith proxies of fish growth. Marine Biology 162, 1019-1031.

757   https://doi.org/10.1007/s00227-015-2645-5

758   Wagenmakers, E., Farrell, S., 2004. AIC model selection using Akaike weights. Psychonomic

759   Bulletin and Review 11, 192-196. https://doi.org/10.3758/Bf03206482

760   Walters, G.E., Wilderbuer, T.K., 2000. Decreasing length at age in a rapidly expanding

761   population of northern rock sole in the eastern Bering Sea and its effect on management advice.

762   Journal of Sea Research 44, 17-26. https://doi.org/10.1016/S1385-1101(00)00045-9

763   Wang, M.Y., Overland, J.E., Bond, N.A., 2010. Climate projections for selected large marine

764   ecosystems. Journal of Marine Systems 79, 258-266.

765   https://doi.org/10.1016/j.jmarsys.2008.11.028

766   Wuenschel, M.J., McElroy, W.D., Oliveira, K., McBride, R.S., 2019. Measuring fish condition:

767   an evaluation of new and old metrics for three species with contrasting life histories. Canadian

768   Journal of Fisheries and Aquatic Sciences 76, 886-903. https://doi.org/10.1139/cjfas-2018-0076

769   Yang, M.S., 1999. The trophic role of Atka mackerel, *Pleurogrammus monopterygius*, in the

770   Aleutian Islands area. Fishery Bulletin, U.S. 97, 1047-1057.

771   Yang, M.S., 2003. Food habits of the important groundfishes in the Aleutian Islands in 1994 and

772   1997. U.S. Department of Commerce, AFSC Processed Rep. 2003-07, Alaska Fisheries Science

773   Center, National Marine Fisheries Service, NOAA, 7600 Sand Point Way NE, Seattle, WA

774   98115, 231 p.

775   Zador, S., Ortiz, I., 2018. Ecoystem Status Report 2018: Aleutian Islands. North Pacific Fishery

776   Management Council, 605 West 4th , Suite 306, Anchorage, Alaska 99501-2252.

777   Zuur, A.F., Ieno, E.N., Smith, G.M., 2007. Analysing ecological data. Springer, New York, New

778   York, 672 pp.

779   Zuur, A.F., Ieno, E.N., Walker, N.J., Saveliev, A.A., Smith, G.M., 2009. Mixed Effects Models

780   and Extensions in Ecology with R. Springer, New York, 574 pp.

781   Table 1. Summary of specimens used to develop Atka mackerel (*Pleurogrammus*

782   *monopterygius*) otolith biochronology.

Collection year	*n* fish	*n* increments	Fish length range (cm)	Fish age range (yr)
1996	48	226	36-48	5-10
1998	18	99	41-43	6-10
2000	32	136	39-46	5-9
2002	33	160	41-47	5-10
2005	43	156	36-45	5-8
2008	28	146	39-43	6-10
2010	34	197	39-46	5-12
2015	53	306	39-47	5-12
Total	289	1426	36-48	5-12

783

784   Table 2. Parameter and variance estimates from most parsimonious full mixed model describing

785   otolith growth of Atka mackerel (*Pleurogrammus monopterygius*).

Fixed effects	Estimate	SE	t
Intercept	-2.721	0.021	-132.279
ln(Age at formation)	-1.065	0.022	-47.515
ln(Age at capture)	0.095	0.045	2.120
Pink salmon abun.	-0.001	0.000	-3.467

Random Effects	Variance	SD	Correlation
Specimen intercept	0.014	0.117	0.230
Specimen slope	0.025	0.159	
Year	0.006	0.075	
Cohort	0.002	0.046	
Residual error	0.036	0.190	

Metric	Value
AIC_c	-235.96
AIC_{wt}	0.62
R^2_m	0.69
R^2_c	0.81

786

787

788   Table 3. Correlations between Atka mackerel (*Pleurogrammus monopterygius*) otolith

789   biochronology (intrinsic mixed model year effect) and biological variables. Significant

790   correlations ($p < 0.05$) are in bold text. L. Copepods and S. Copepods are large and small

791   copepods, respectively.

	Otolith	Condition	L. Copepods	S. Copepods	Euphausiids	Salmon
Otolith	1					
Condition	-0.19	1				
L. Copepods	**0.58**	-0.27	1			
S. Copepods	**-0.58**	-0.11	-0.28	1		
Euphausiids	0.24	0.02	-0.05	-0.20	1	
Salmon	**-0.52**	-0.08	**-0.73**	0.35	0.07	1

792
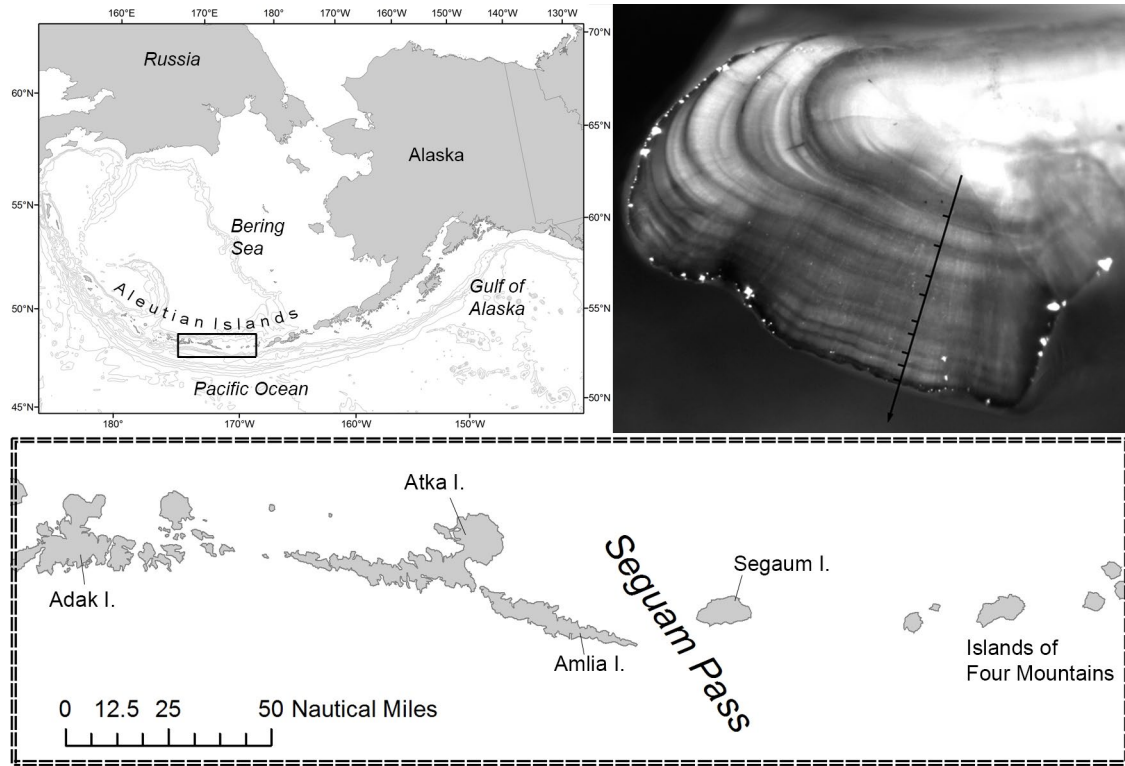
Figure 1. Counter-clockwise from top left: Map of Aleutian Islands and surrounding waters, close-up of Seguam Pass study area (inside black box). Actual collection locations cannot be shown due to vessel confidentiality agreements. Transverse section of an Atka mackerel (*Pleurogrammus monopterygius*) otolith showing axis of measurement and demarcation of growth increments. Note alternating pattern of wide and narrow increments.
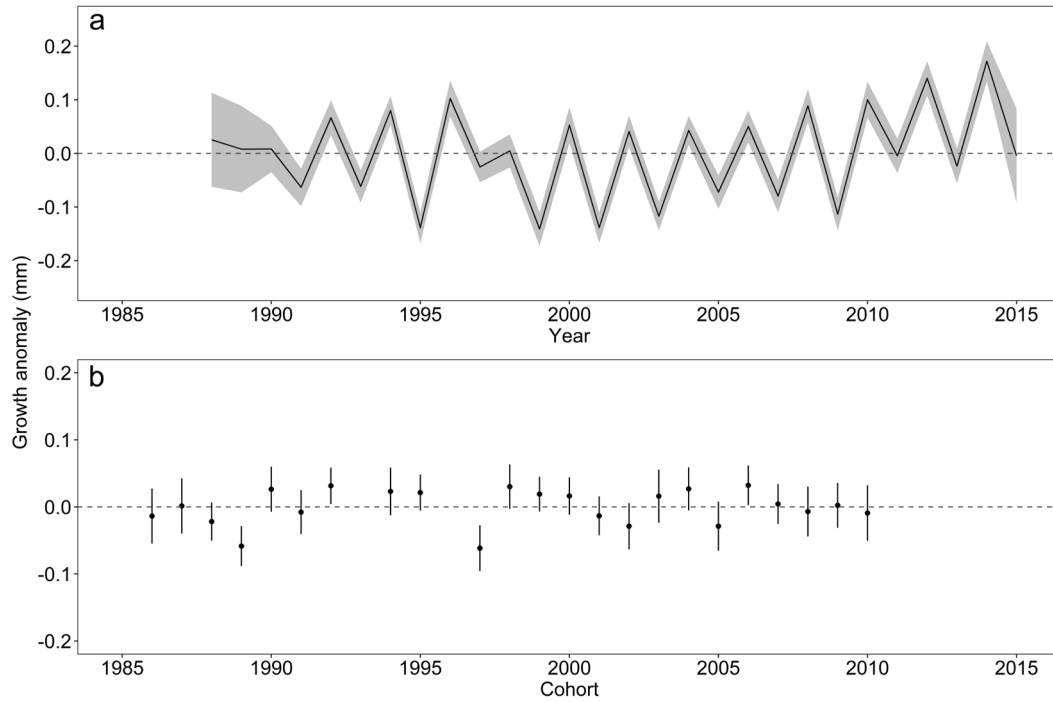
800
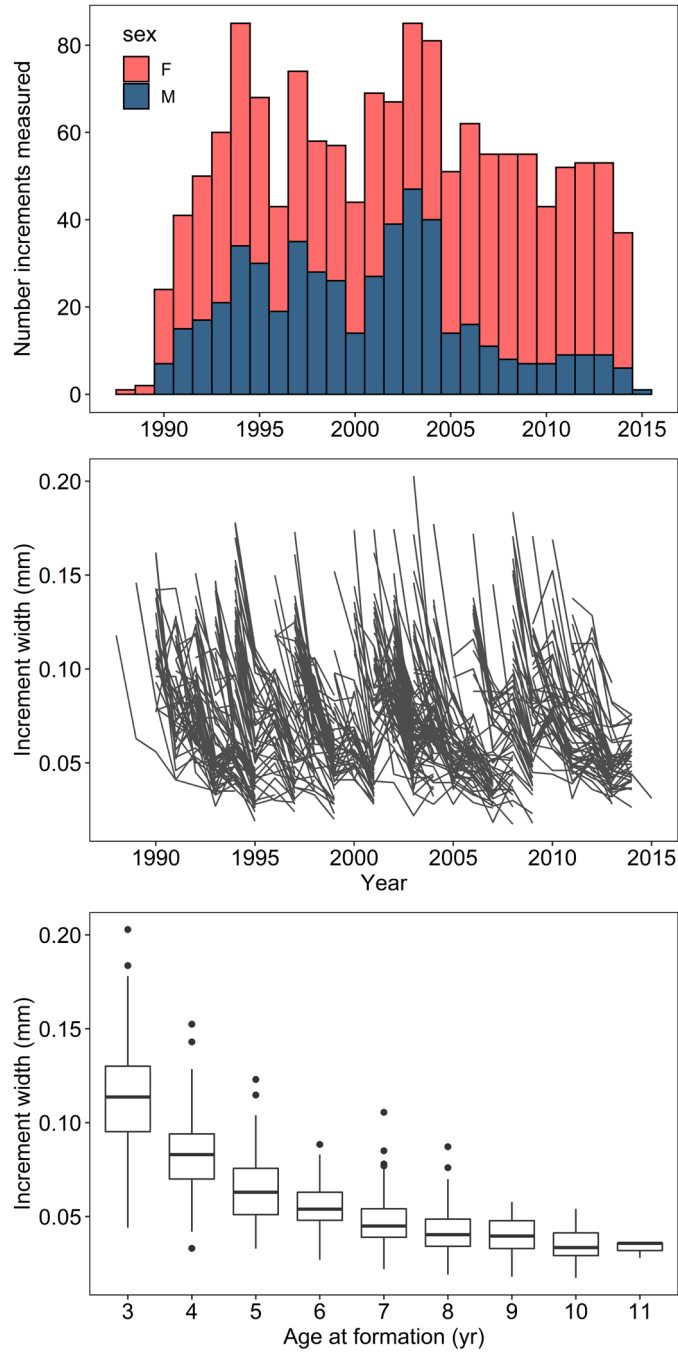
Figure 2. Atka mackerel (*Pleurogrammus monopterygius*) otolith biochronology sample depth

(top; males are in blue and females are in coral), raw growth increment measurements (middle),

and decline in increment width relative to age at formation (bottom).

804

Figure 3. Otolith growth anomalies of Atka mackerel (*Pleurogrammus monopterygius*) predicted

by the most parsimonious intrinsic mixed effect model. a) Annual variation in growth (year

effect or "biochronology", black line, with standard error represented by shaded area), and b)

cohort-specific growth variation (points, with standard error represented by bars), after effects of

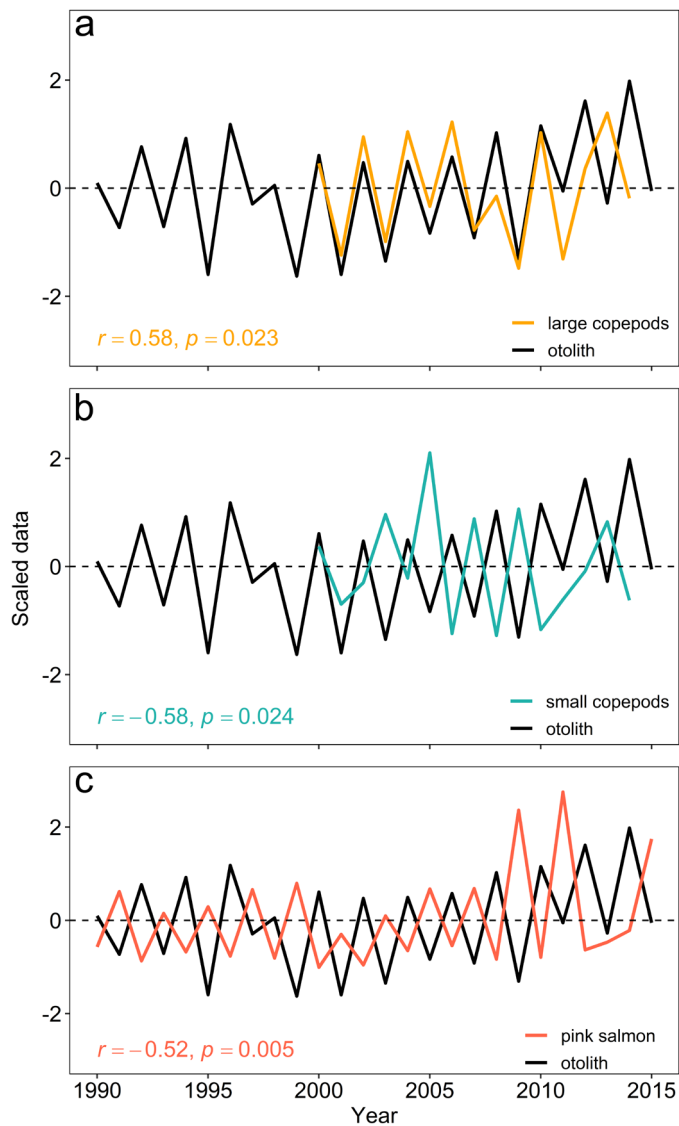fish age at increment formation and age at capture have been removed.
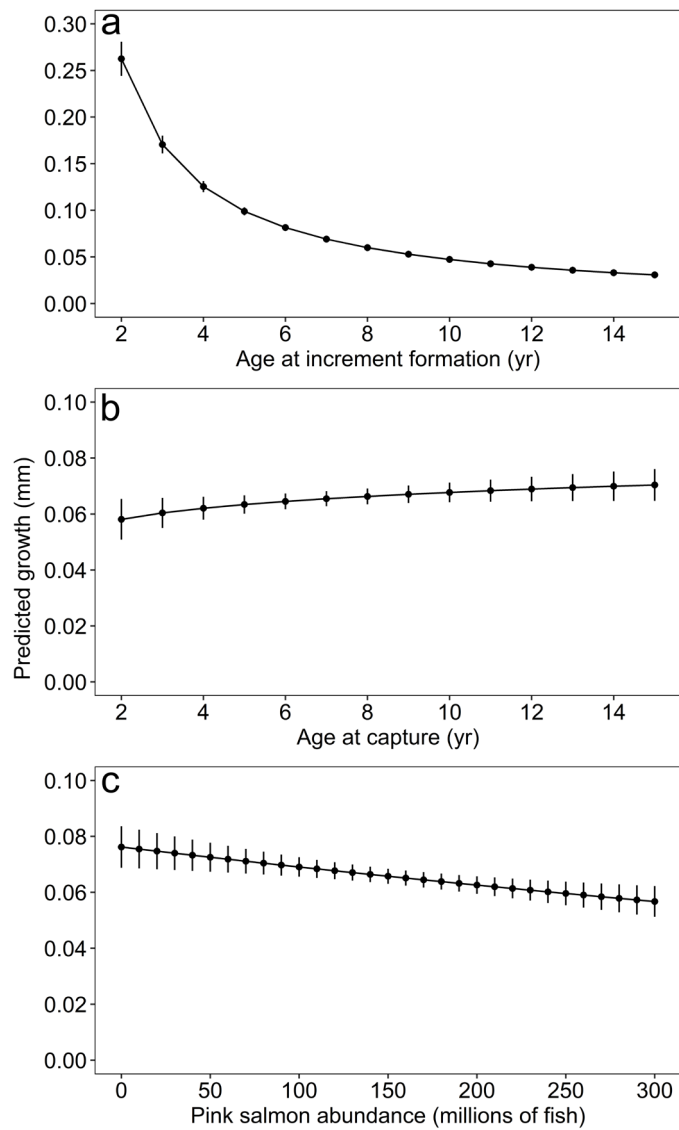
812

813　　Figure 4. Effects of a) fish age at increment formation, b) fish age at capture, and c) pink salmon

814　　abundance on otolith growth of Atka mackerel (*Pleurogrammus monopterygius*). Points

815　　represent means and bars represent 95% confidence intervals.

816

817

818 Figure 5. Biological time series significantly correlated (*p* < 0.05) with the Atka mackerel

819 (*Pleurogrammus monopterygius*) otolith biochronology (year effect from intrinsic mixed effects

820 model): a) large copepod abundance, b) small copepod abundance, and c) pink salmon

821 abundance. All data have been standardized to a mean of 0 and standard deviation of 1.

822

823

824   Appendix Table A.1. Results of model fitting for the optimal extrinsic fixed effects structure

825   describing growth of Atka mackerel (*Pleurogrammus monopterygius*) otolith increments. All

826   extrinsic models share the same random effects and intrinsic fixed effects structure (see main text

827   for details). Extrinsic fixed effects considered in the model set are Atka mackerel abundance

828   index (Atka), pink salmon (*Oncorhynchus gorbuscha*) abundance (Pink), and sea surface

829   temperature (Temp). K = number of parameters, AIC_c = Akaike Information Criterion corrected

830   for small sample sizes, Δ_i = difference between each model's AIC_c and the model with the

831   minimum AIC_c, AIC_{wt} = Akaike weight, and LL = log-likelihood.

832

Extrinsic fixed effects	K	AIC_c	Δ_i	AIC_{wt}	LL
None	9	-228.17	7.79	0.01	123.15
Atka	10	-226.37	9.59	0.01	123.26
Pink	**10**	**-235.96**	**0**	**0.62**	**128.06**
Temp	10	-226.44	9.51	0.01	123.30
Atka + Temp	11	-224.76	11.20	0.00	123.47
Pink + Temp	11	-234.16	1.80	0.25	128.17
Atka + Pink + Temp	12	-232.47	3.49	0.11	128.34

833
834

835

836